

Elastic Strength and Anisotropy of the Continental Lithosphere of India

JIMMY STEPHEN*

National Geophysical Research Institute, Hyderabad-500 007

(Received 5 December 2005; Accepted 17 August 2006)

Elastic strength of the Indian lithosphere is reviewed in this paper giving emphasis to the estimation of effective elastic thickness (T_e) and its azimuthal variation showing the major weakness directions in the lithosphere. The estimations were carried out using advanced 2D multitaper (MTM) and mirrored periodogram (MPM) spectral based Bouguer gravity and topography coherence analysis and a comparison is made. These estimates differ considerably yielding an exaggerated T_e from the MPM. However, both these estimations evidenced relatively low elastic strength for the entire Indian lithosphere compared to many other parts of the world. The study also depicts a noticeable variation across the central Indian tectonic zone, which acts as a major divide in the Indian shield. A higher T_e range (20-25 km) is obtained for the northern region than the southern region (12-16 km). These values are almost in agreement with the prevailing earthquake focal depths, where there is more shallow earthquakes in the south than the north. This suggests that the elastic thickness is nearly confined within the seismogenic thickness. The present anisotropic results are in good agreement with the stress orientations in the north depicting the plate movement directions, whereas scattered in the south.

Key Words: Effective elastic thickness, coherence anisotropy, Indian lithosphere, gravity, topography, multitaper, periodogram

Introduction

The isostatic response of the Earth's lithosphere can be studied better on the basis of the long-term accommodation of topographic loading at various interfaces. Considering the lithosphere as a thin elastic plate, the flexure due to surface topography and subsurface density load deforms the Moho and can thus be inferred from gravity anomalies. It is understood that in the case of a fully compensated mountain root, it is a state of near-Airy isostasy that corresponds to a lithosphere with no strength or zero thickness [1]. In this case the free-air gravity anomaly is small and approaches zero for the longest wavelengths, and the Bouguer gravity anomaly is nonzero, reflecting the crustal root. Generally, the Bouguer anomaly is strongly correlated with the topography at long wavelengths. Whereas in the case of short wavelengths, the lithosphere is assumed to have more rigidity or strength and can support topographic loads without any significant compensating crustal root. Therefore, the correlation of Bouguer anomaly with topography, which is wavelength dependent, could yield the transition from compensated to uncompensated topography. For a rigid lithosphere the transition occurs at longer wavelengths [2]. This paper presents the elastic strength and its anisotropy in the continental lithosphere of India, calculated on the basis of transfer function relationships between gravity and topography fields. The estimations were made using a 2D multitaper coherence analysis.

The elastic strength of the lithosphere can be quantified by its flexural rigidity (D) or effective elastic thickness (T_e). It has been found that generally T_e varies over a wide range [3, 4]. Earlier studies provide high values of T_e , with a general picture that cratons are having $T_e > 50$ km. But later it has been shown on the basis of focal depths of earthquakes under continents (always < 30 km) and 450°C isotherms (which corresponds to T_e in oceanic regions) shallower than 50 km, that T_e for stable continental regions should not be expected to exceed 25 km [5]. T_e can be determined either by modeling the gravity and topography data together, or by using statistical methods, to estimate the admittance [6, 7] and coherence [8] of the two data sets from their cross spectra. Recent studies on the isotropic mechanical behaviour of the lithosphere provide insights into the structure and deformation of the lithosphere [5, 9, 10, 11]. Moreover, it can compliment the seismic anisotropy studies, which inspired the hypothesis of vertically coherent deformation on the basis of shear-wave splitting measurement correlated to the geologic deformation indicators measured at the surface.

The azimuthal variations in the gravity and topography coherence functions also provide an opportunity to understand the anisotropic conditions in the lithosphere. The studies show that a regime of "fossil" deformation overlies a zone characterized by a predominant influence of present-day mantle deformation. In other words, the lithospheric anisotropy

* Present address: 206 – 3360 Paul Anka Dr, Ottawa, ON, K1V9S2, Canada
e-mail: jimstep@yahoo.ca

is predominantly caused by strain fossilized in the subcontinental mantle since the last major episode of tectonic activity, rather than current mantle deformation [12, 13]. This dominant fossil strain field of the lithosphere can be inferred from the orientation of gravity anomalies in relation to the topography, which can do in the spectral domain by extracting the azimuthal variation of the gravity-topography coherence function. This new approach gives stress to the concept of mechanical anisotropy [10], which is also a geologically agreed concept [14, 15].

Te Estimates for the Indian Continent

Previous Effective Elastic Thickness (T_e) estimates for the Indian continent yielded a wide spectrum of T_e values: 100 km for Deccan volcanics studied with a migrating volcanic load model [16], 13-61 km for Indian peninsula from free air admittance [5], 8-12 km for Deccan volcanics from 1D free air admittance and Bouguer coherence [17] and 15 km for Kerala-Konkan margin [18] from backstripping / backstacking analysis. Two dimensional multitaper based estimations were further carried out for the Eastern Himalayan-Tibetan Plateau, yielding a T_e range of 20-35 km [19]. A detailed

investigation for the South Indian shield with a comparison of earlier mirrored periodogram to the recent multitaper method has been provided by Stephen et al. [20]. Most recently, the estimations based on advanced spectral methods proved that the Indian lithosphere is mechanically weaker than many other parts of the world [21]. Also, a noticeable strength variation is evidenced across the central Indian tectonic zone, supporting its Proterozoic collisional tectonics [22]. In another attempt, Rajesh and Mishra [23] retrieve the lithospheric thicknesses for different cratons, based on the transitional wavelengths of gravity-topography coherence.

Tectonic Settings

The Indian plate characterizes numerous continental and oceanic fragments that carry imprints from early Archaean crustal evolution to present day tectonics (Fig. 1). Its continental lithosphere is presumed to have developed around certain Archaean cratonic nuclei such as Dharwar, Bundelkhand, Bastar and Singhbhum, which were surrounded by and/or sutured along Proterozoic mobile belts. About two-third of the surface exposure of the Indian peninsula consists of Precambrian rocks, extending through the entire range of Precambrian time, from 3,400 Ma to the late Precambrian / early Paleozoic.

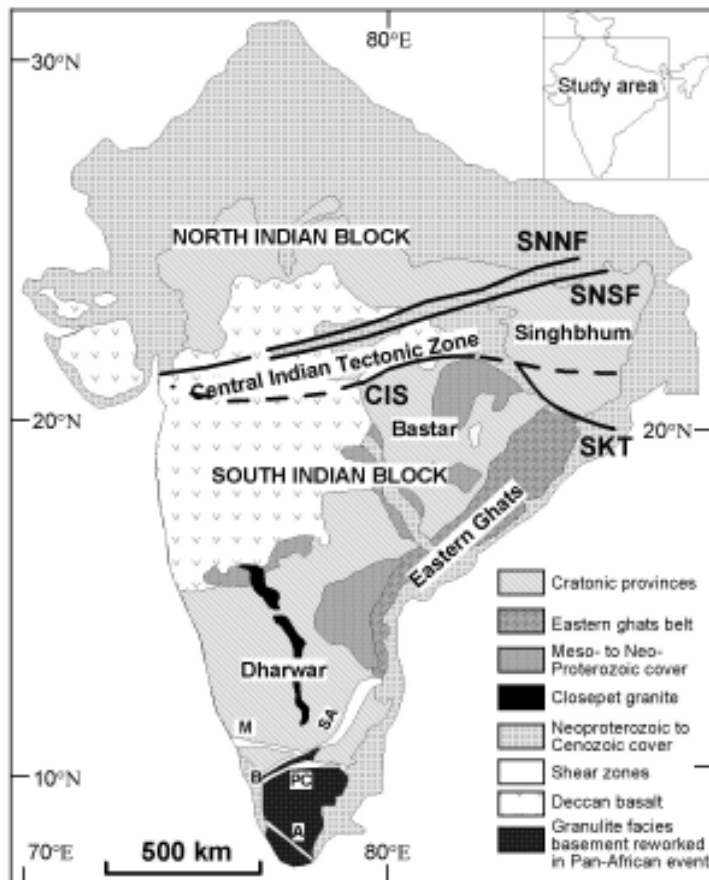


Fig. 1: Geological map of India showing different tectonic provinces, giving emphasis to the Central Indian Tectonic Zone (CITZ) dividing the northern and southern regions (modified after Zhao et al. [24]). SNNF – Son-Narmada North ault, SNSF – Son-Narmada South Fault, SKT – Sukinda Thrust, CIS – Central Indian Suture, m, B, SA, PC and A are Moyar, Bhavani, Salem-Attur, Palghat-Cauvery and Achankovil shear zones respectively

The presence of exposed / covered Archaean provinces, Proterozoic sedimentary and volcano-sedimentary basins, exposed and covered basaltic provinces, and the zone of ongoing continental convergence are the major characteristics of the Shield. The ENE-WSW trending Central Indian Suture (CIS) assumes a major divide in the shield, with resulting northern and southern blocks. The Central Indian Tectonic Zone (CITZ), which forms a wide zone immediate north of the CIS, characterizes a collage of different lithotectonic terrains ranging in age from Archaean to Recent. It is bounded by Son-Narmada North Fault in the north and the CIS in the south, forming ~200 km wide tectonic zone. The tectonothermal evolutionary history of the CITZ has become a subject of recent interest [25, 26, 27]. An elastic strength variation across the CITZ was suggested by Stephen [28].

Data for Te Estimation

Bouguer gravity and topography data were used for the present analysis. Reasonable accuracy necessary for the present analysis is ensured in the gravity field by merging various data sets [29, 30, 31, 32, 33, 34, 35, 36, 17, 37] to the available 10 mGal map of India [38]. The bias in

the gravity field due to the long-wavelength central Indian Ocean geoidal low caused from deep-seated sources [39] is removed based on calculations by Subba Rao [40], since any isostatic studies with an areal extent less than its characteristic wavelength is insignificant. The merged geoidal corrected Bouguer gravity field is shown in Figure 2. Figure 3 shows the topography image over the Indian region, which is extracted from the global GTOPO-30 database [41]. Both gravity and topography data were further interpolated to retain a minimum resolvable (Nyquist) wavelength of 8 km.

The other input parameters used in the calculation of theoretical models to enable a T_e inversion process are Poisson's ratio (σ), Young's modulus (E), average crustal density (ρ_c), mantle density (ρ_m) and the crustal thickness. These values need to be fixed for each data windows. In this study, σ , E , ρ_c and ρ_m were chosen to be 0.25, 10^{11} N/m², 2.7 kg/m³, and 3300 kg/m³, respectively. Since topographic loading and one interface of subsurface loading (at Moho) were considered for all inversions, the average crustal thickness values were constrained from available deep seismic sounding (DSS) profiles [42, 43]. In regions where DSS profiles are not

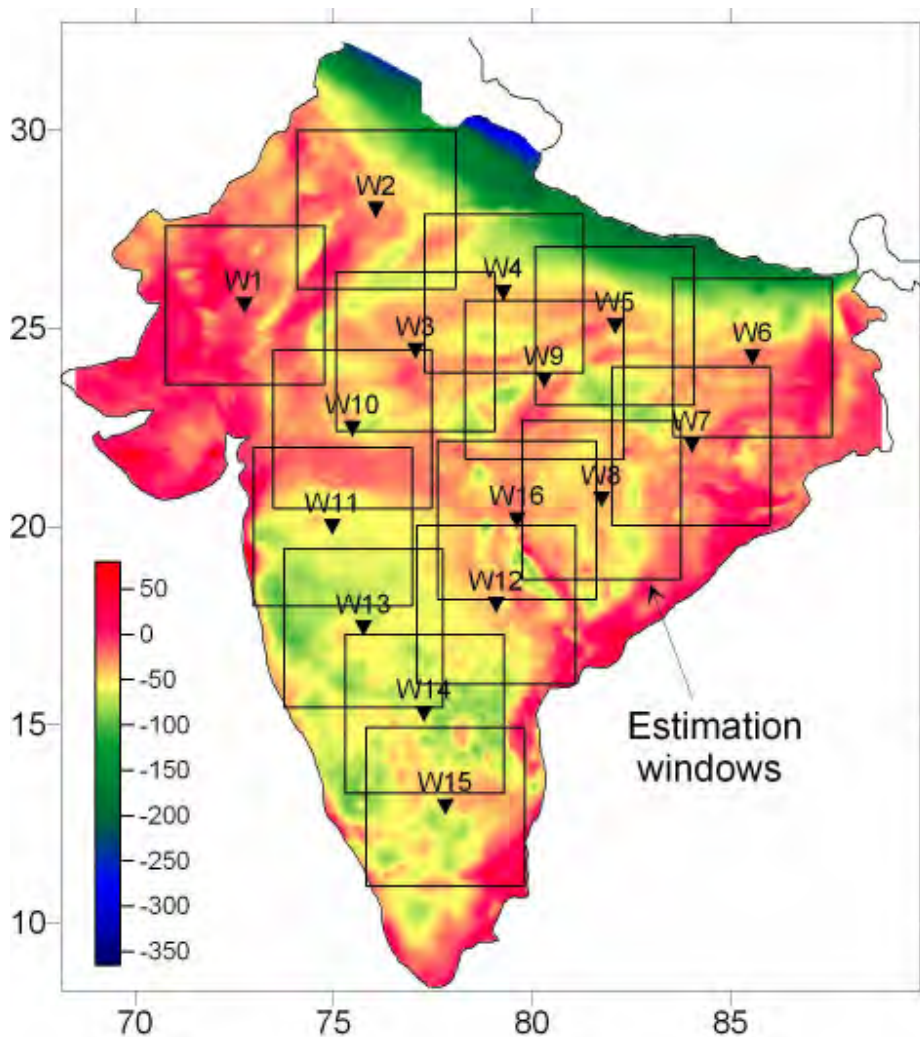


Fig. 2: Geoidal corrected Bouguer gravity field over Indian shield, superimposed with the windows used for present T_e estimation

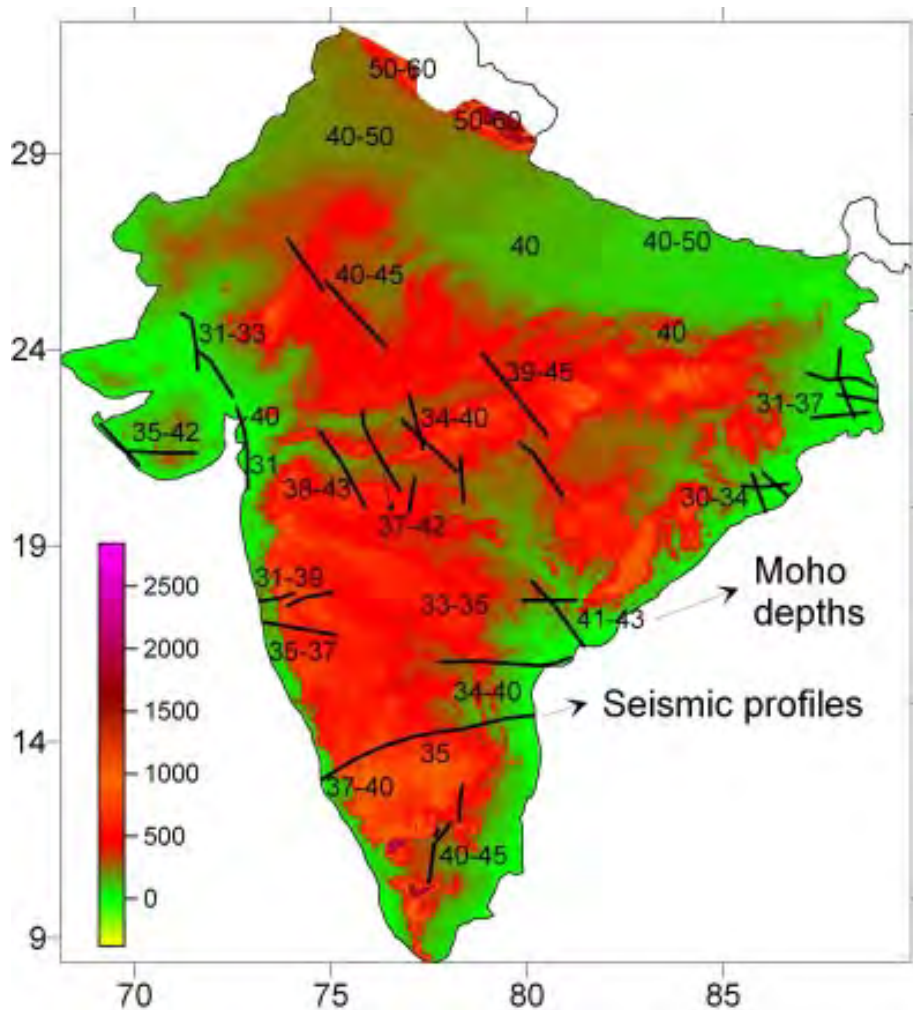


Fig. 3: Topographic image over Indian shield. Superimposed solid lines are the deep seismic sounding profiles available in the region, shown with the crustal thickness ranges

available, average values were taken from tele-seismic receiver function analysis [44] and fundamental mode Rayleigh and Love wave studies [45]. Considering a window size of $4^{\circ} \times 4^{\circ}$ ($\sim 440 \times 440 \text{ km}^2$), any local perturbations in the Moho depths were considered to be outliers in the present T_e estimation and therefore neglected.

Methodology

As discussed earlier, T_e is usually determined from the transfer function relationships between gravity and topography. Usually the admittance and coherence functions are used to invert for T_e . The wide spectrum of variation in earlier T_e estimations over the continents was subjected to the bias due to different spectral estimation schemes. The present study is carried out using the Bouguer gravity and topography coherence method, which could effectively address the subsurface loading problems. Coherence function is a measure of the consistency of the phase relationship between individual measurements of a particular Fourier component, independent of its magnitude. It is a wavenumber domain analogue of correlation, and

suggests a way of synthesizing two fields with a known coherence [46]. Long-wavelength topography will usually be compensated by a deflection commonly assumed to occur at the Moho, giving a high coherence between topography and Bouguer anomalies. If in addition, a statistically independent process causes loading in the subsurface, the lithosphere will be again characterized by a high coherence. Whereas, there will not be any coherence at short wavelengths, since the topographic and subsurface loads are supported largely by stresses within the plate. Therefore the transition wavelength between a coherent and an incoherent relationship is diagnostic of the flexural rigidity.

In this study, the T_e estimations are made using an advanced 2-dimensional Thomson-Slepian multitaper (MTM) method [47] and a mirrored periodogram (MPM) method [9] of Coherence analysis. Recent studies have proved that the multitaper-based coherence analysis yields better T_e estimates [48, 49], however, here I present both the results to make a comparison. In the case of MPM, the data grid is mirrored along both the x and y directions. Here no window was applied; the

periodogram method was applied on the mirrored data and the obtained data grid is assumed to be periodic. But any deviations from flat ends in the grid will result in spectral leakage and the phase information will be lost. These distortions in turn result in a shift of the coherence functions to smaller wave numbers, causing overestimation of T_e . On the other hand, MTM offers improved power spectral density estimates with greatest leakage resistance, minimum bias and have well-behaved estimation variance. It uses optimal FIR filters, known as discrete prolate spheroidal sequences (DPSS) or Slepian sequences [50], rather than a single box window. The use of only one taper results in the loss of much information, whereas the use of a complete set of eigentapers, the information is extracted evenly from all samples. Use of a time-bandwidth product (NW) balances the variance and resolution and in turn determines the number of useful tapers (2NW-1) to form the estimate. In the present study, I use 2D data tapers, capable of giving reliable 2D coherence estimates.

The effective elastic thickness inversions were carried out for all the data windows shown in Figure 2, with a $4^\circ \times 4^\circ$ size centered over the shown points. These identical ($\sim 440 \times 440 \text{ km}^2$) square windows were chosen to obtain the unbiased T_e variation of the shield, and to retain the uniformity in both the x and y co-ordinates for the analysis of 2D windows, and hence to allow a comparative study. The ability of this window size to capture elastic behaviour of the Indian lithosphere has been earlier studied [20]. In addition, the 2D multitaper method was used to extract the azimuthal variation of gravity-topography coherence functions in the spectral domain, which reflects the dominant mechanical weakness directions. Isostatic compensation involves all of the elastic lithosphere, and the isostatic response thus represents the time- and depth-integrated dominant mode of deformation. This interpretation is not unique, as we need to assume that the observed topography and gravity are in static equilibrium with each other. However, studies show that the 2D multitaper method gives better estimation, since it will not obliterate the directionality in the signal [10].

Results and Discussions

T_e and its Anisotropy

T_e inversions were carried out with both the multitaper (MTM) and mirrored periodogram (MPM) based coherence methods, and a comparison is made (Figs. 4 and 5). MTM yielded a T_e range of 12-25 km for the Indian lithosphere, whereas the MPM yielded almost

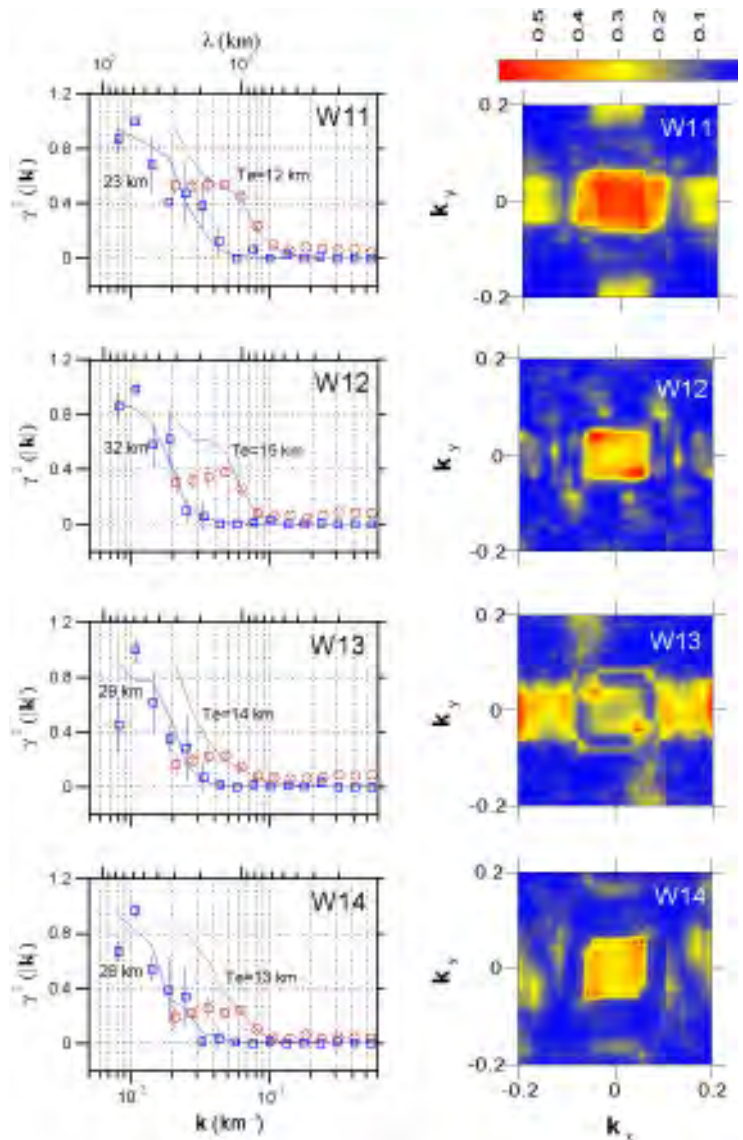


Fig. 4: Coherence estimates for 4 selected windows in the southern region. Azimuthally averaged multitaper and mirrored periodogram T_e inversions are shown in red and blue colours respectively (left). Images in the right column shows the multitaper based 2D coherence anisotropy for these windows

twice the values (23-40 km). This exaggerated T_e estimates from MPM based inversions are not unusual and is similar to results over the Australian continent [10]. Therefore I give more emphasis to the discussions on multitaper estimations in this paper. Indian Shield evidenced very low T_e values from MTM compared to similar estimations for other parts of the world. Figure 6 shows the proposed T_e map for the Indian continent. The map shows a clear strength variation between the northern and southern regions, separated by the Central Indian Tectonic Zone.

The southern region of Indian lithosphere appears to be mechanically weaker than the northern region with values ranging from 12 to 16 km. Northern region give values of 18-25 km. 2D coherence anisotropy evidenced scattered orientations in the south, but likely to match

the stress orientations towards the north. This nearly N-S oriented coherence anisotropy is indicative of the plate movement directions (shown in Figure 5 for windows W2, W4 and W5). This orientation is in well agreement with the earlier N-S anisotropy reported for Eastern Himalayan-Tibetan region. On contrary, most of the southern data windows do not show any prominent anisotropic directions, except the E-W orientations obtained over the Deccan Volcanic province towards the north-west (shown as W11 & W13 in Figure 4). Stephen et al. [20] have earlier reported the low T_e and absence of any notable coherence anisotropy in the south Indian region. The anisotropic orientations are shown in Figure 7.

Coherence Anisotropy and Stress Orientations

Direction of both compressive and extensional tectonic stress lower T_e values in the same direction [51]. In the Indian Shield, three stress provinces were identified [52]: (1) the mid-continent province with mean stress orientation in the NE direction, sub-parallel to the direction of compression due to resistive forces at the Himalayan collision zone, (2) Bengal province with E-W orientations and (3) the southern province, generally scattered, with a rough NW orientation similar to that in the Central Indian Ocean. SIB is devoid of any coherence anisotropy, except the prominent E-W directions seen in its northwestern part. However, in NIB it follows good relationship with the stress orientations. Especially the northern region exhibits very clear N-S (and also NE) weakness directions. The E-W stress orientation in the Bengal Basin province is also retrieved in the coherence anisotropy (shown in the data window 7).

Coherence and Seismic Anisotropies

The coherence anisotropy and the seismic anisotropy can be correlated [11]. Seismic anisotropy is an indicative of the lattice preferred orientation (LPO) of anisotropic mantle minerals, caused due to finite strain. In the case of continental collision, the fast polarization direction of SKS splitting is expected to be parallel to the structural trends or nearly perpendicular to the compression direction. In the Indian Shield, the seismic anisotropic studies are too meager to make any valid correlation. Only a rough relation is obtained in the northwestern part of SIB. The absence of any dominant anisotropic directions in the southern region is in agreement with the earlier seismic anisotropy studies beneath the

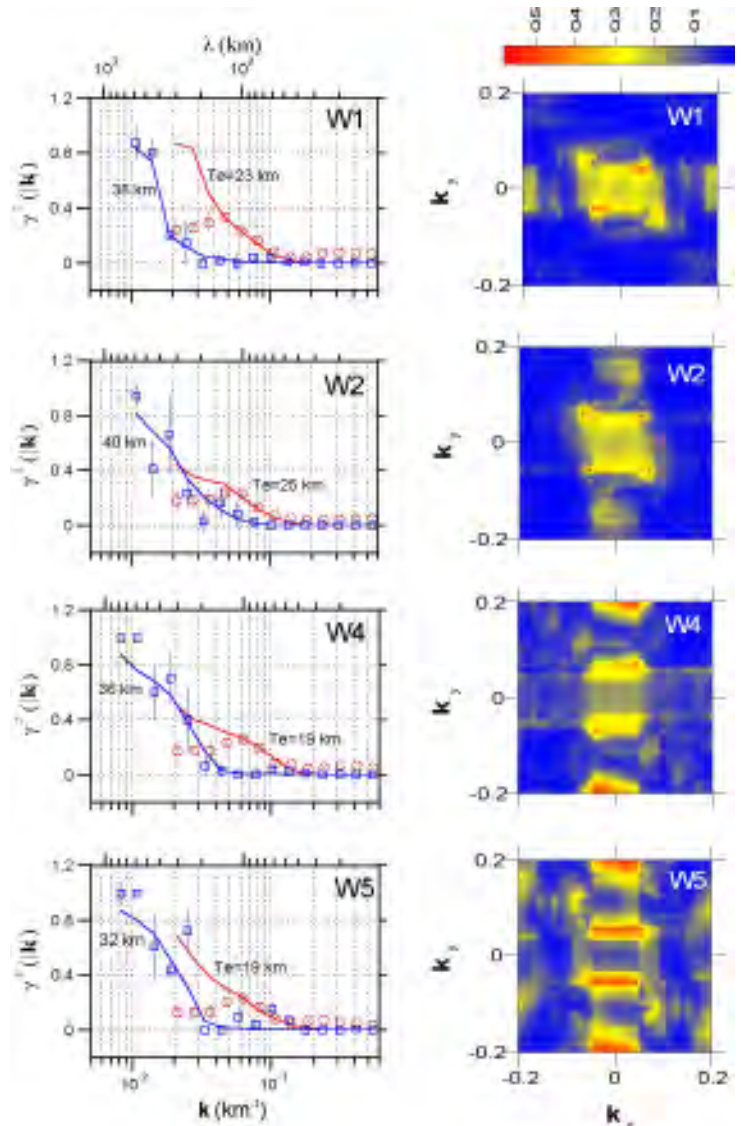


Fig. 5: Coherence estimates for selected windows in the northern region. Explanations are same as in Figure 4

Geoscope station at Hyderabad, which evidenced no detectable anisotropy [53].

T_e and T_s Correlation

As discussed earlier, T_e evidenced wide spectrum of variation in the continents and many correlations were made to obtain physical meaning to the estimations. One of the major concern was to see how well T_e could be correlated with thickness of the seismogenic layer (T_s). Recently different thoughts were emanated: a few suggested T_e is close to T_s , where the strength of lithosphere resides within the T_s , while others argued that T_e is much higher, reflecting the integrated brittle, elastic and ductile strength of the lithosphere. Based on the coherence analysis method of Forsyth [8] T_e values in excess of 100 km, about 4-5 times greater than the seismogenic thickness (T_s), have been obtained over old inactive shields. McKenzie and Fairhead [5] concluded

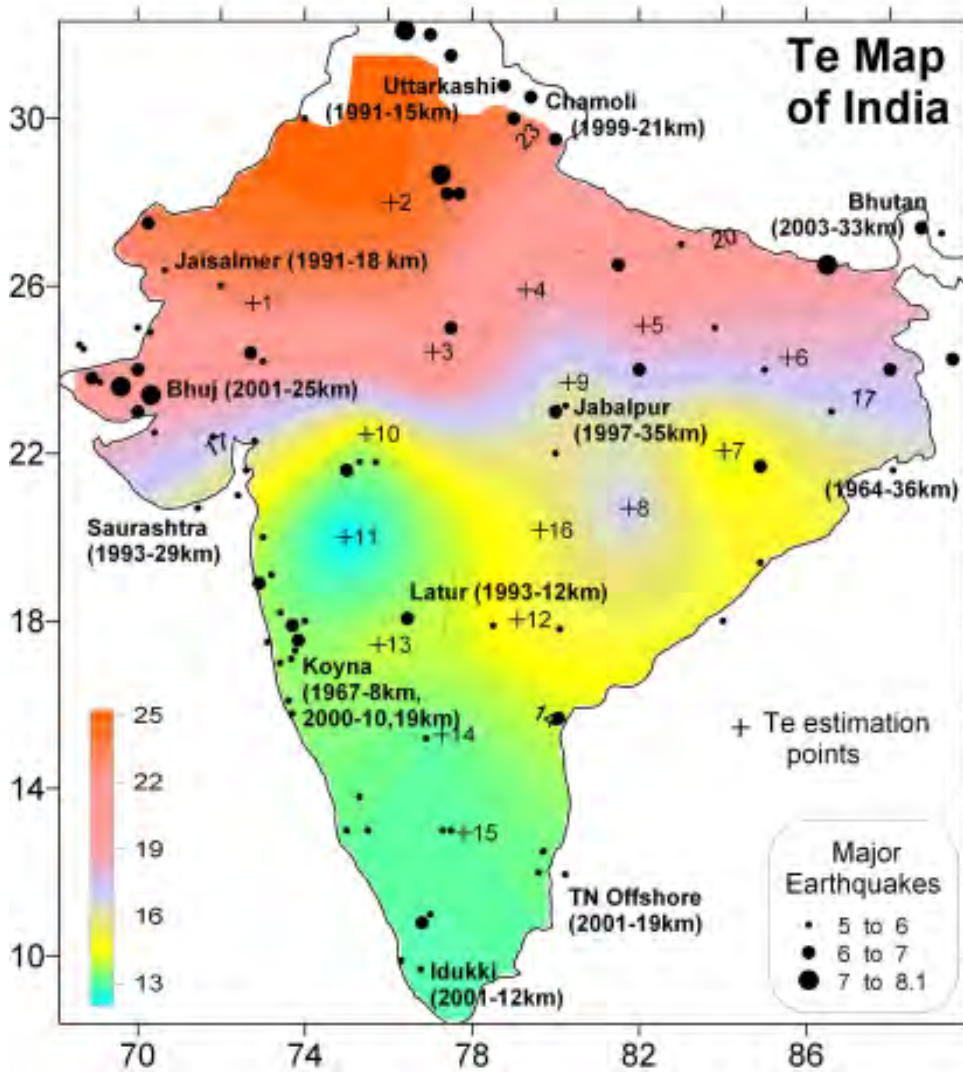


Fig. 6: *Te* Map of India, superimposed with the earthquake distribution, $M > 5.0$ [55, 56, 45]. Focal depth values and year of occurrence are shown for few significant earthquakes

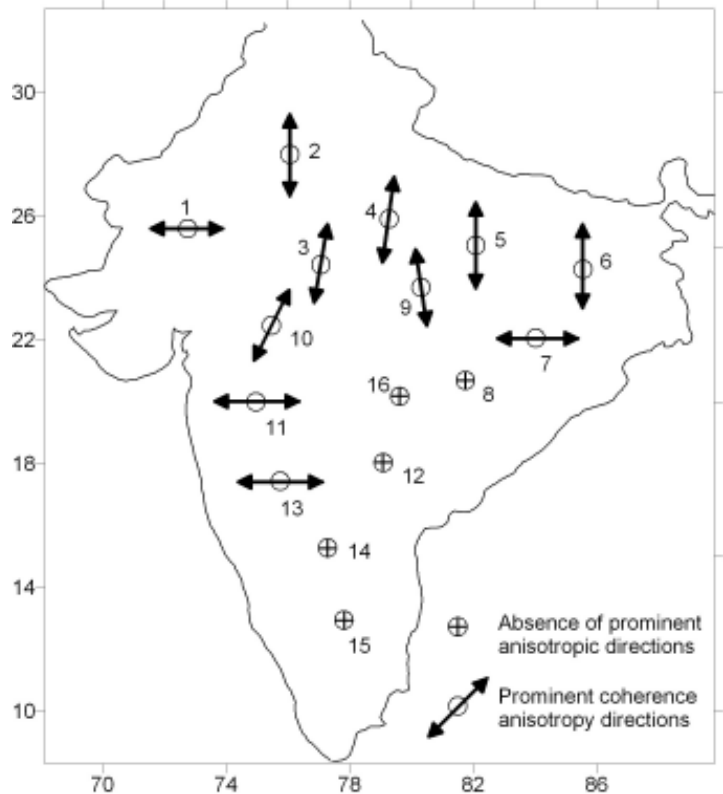


Fig. 7. Major mechanical anisotropic directions estimated for the Indian lithosphere, from 2D multitaper coherence analysis

on the basis of free air admittance and Bouguer coherence methods that T_e rarely exceeds T_s , which was further substantiated by Maggi *et al.* [54]. Previous T_e estimates over peninsular India have yielded a wide spectrum, ranging 8-100 km, studied with migrating volcanic load model [16], and free air admittance and Bouguer coherence analysis [5, 17]. However, the present study yields a first order correlation between T_e and T_s in the Indian Shield. Figure 6 shows the distribution of significant earthquakes superimposed over the T_e map of India.

The available earthquake focal depth data also shows a difference between the northern and southern regions. The southern region characterizes relatively shallow focus earthquakes, compared to the depth of occurrence in the northern region. The T_e values in the south, almost coincident with the upper crustal thickness, suggests that its lithospheric strength is mostly confined in the upper crust. On the other hand, the higher T_e obtained in the north suggests its lithospheric strength contribution from both upper and parts of lower crusts. The brittle-ductile transition is also important, since it gives a correlation with the depth of seismicity. The low mantle heat flux calculated for the Jabalpur earthquake occurred at a depth of 35 km, suggests a relatively cooler and brittle lower crust [57]. However, the seismogenesis of stable continental region (SCR) earthquakes show different source mechanisms, as evidenced in Kachchh, Kilari and Jabalpur earthquakes [58]. Also, it is to be noted that the nucleation of lower crustal earthquakes need not necessarily discard the ductile nature at that depth, since the instabilities in ductile flow itself may act as nuclei for deep crustal earthquakes [48]. The T_e extending to the lower crustal layers observed in the Northern block of the Indian shield suggests a possibility that the lower crust contributing even more strength than the upper mantle and support the surface and subsurface loads, at least in some parts of the shield.

Conclusions

Relatively low values of effective elastic thickness, T_e were obtained for the entire Indian Shield from the multitaper based coherence analysis method. Also, substantial T_e variation has been mapped between the north and southern shield regions joined along the central Indian tectonic zone, with T_e increasing towards the north (12-16 km for SIB and 18-25 km for NIB). The mirrored periodogram method yielded somewhat exaggerated T_e values for all the analyzed windows. However, the transition between northern and southern blocks is evident in these estimates too with values ranging 32-40 km for the northern block and 23-32 km for the southern block. Present results of low elastic thickness shows that the strength of the Indian lithosphere resides within the

average earthquake focal depths. In the southern region it has been even confined in the upper crust, while parts of lower crust contribute to the strength in the northern region. The variation in T_e from south to north is also reflected with an increase in the depth of occurrence of earthquakes.

T_e and the depth of average occurrence of earthquakes, T_s in the Indian Shield follows a rough correlation, suggesting that the strength of the lithosphere resides within the seismogenic layer. The variation in T_e from south to north is also reflected in the T_s , with relatively deeper earthquakes occur in the north. The 2D coherence calculations yielded its anisotropic conditions (or the mechanical weakness directions) in the Indian Shield. Except in the southern regions, the coherence anisotropy is well correlated with the maximum horizontal stress orientations obtained from various stress indicators. In the south, more or less scattered stress directions and the absence of any prominent coherence anisotropy were evidenced.

Acknowledgements

I express my deep gratitude towards Indian National Science Academy, New Delhi for selecting me for the award of INSA Young Scientist Medal for the year 2005. I sincerely thank Prof RN Singh, Dr VP Dimri and Dr B M Reddy for their encouragement. I also thank Dr SB Singh and other scientists of NGRI for their constant support.

References

1. D L Turcotte and G Schubert *Geodynamics Application of Continuum Physics to Geological Problems John Wiley New York* (1982)
2. G D Karner *BMR J Aust Geol Geophys* **7** (1982) 55-62
3. M K McNutt, M Diament and M G Kogan *J Geophys Res* **93** (1988) 8825-8838
4. A B Watts *Isostasy and Flexure of the Lithosphere Cambridge University Press UK* (2001) 458p
5. D P McKenzie and J D Fairhead *J Geophys Res* **102** (1997) 27523-27552
6. L M Dorman and B T R Lewis *J Geophys Res* **75** (1970) 3357-3365
7. D P McKenzie and C Bowin *J Geophys Res* **81** (1976) 1903-1915
8. D W Forsyth *J Geophys Res* **90** (1985) 12623-12632
9. M T Zuber, T D Bechtel and D W Forsyth *J Geophys Res* **94** (1989) 9353-9367
10. F J Simons, M T Zuber and J Korenaga *J Geophys Res* **105** (2000) 19163-19184
11. F J Simons, R D van der Hilst and M T Zuber *J Geophys Res* **108** (2003) 2250 doi: 10. 1029 / 2001JB000704
12. L P Vinnik, R W E Green and L O Nicolaysen *Nature* **375** (1995) 50-52
13. P G Silver and W Chan *J Geophys Res* **96** (1991) 16429-16454
14. A Vauchez, A Tommasi and G Barruol *Tectonophysics* **296** (1998) 61-86

15. A Tommasi and A Vauchez *Earth Planet Sci Lett* **185** (2001) 199-210
16. A B Watts and K G Cox *Earth Planet Sci Lett* **93** (1989) 85-97
17. V M Tiwari and D C Mishra *Earth Planet Sci Lett* **171** (1999) 289-299
18. S Chand and C Subrahmanyam *Earth Planet Sci Lett* **210** (2003) 317-332
19. R S Rajesh, J Stephen and D C Mishra *Geophys Res Lett* **30** (2003) 1060 doi:10.1029/2002GL016104
20. J Stephen, S B Singh and D B Yedekar *Geophys Res Lett* **30** (2003) 1853 doi:10.1029/2003GL017686
21. J Stephen (Abst) *ISCA Young Scientist programme Ahmedabad* (2005)
22. J Stephen, S B Singh and D B Yedekar *Current Science* **89** (2005) 190-195
23. R S Rajesh and D C Mishra *Earth Planet Sci Lett* **225** (2005) 319-328
24. G Zhao, M Sun and S A Wilde *Precambrian Res* **122** (2003) 201-233
25. S K Acharyya and A Roy *J Geol Soc India* **55** (2000) 239-256
26. A Roy and M H Prasad *Geol Surv India Spl Publ* **64** (2001) 177-197
27. S K Acharyya *Gond Geol Magz Spl Vol 7* (2003) 9-31
28. J Stephen *South Indian shield lithosphere: Its mechanical strength and anisotropy* Thesis submitted to SRTM University Nanded (2003) 180p
29. K L Kaila, H C Tewari and D M Mall *J Geol Soc India* **29** (1987) 293-308
30. R K Verma and P Banerjee *Tectonophysics* **202** (1992) 375-397
31. N K Brahmam *Current Science* **64** (1993) 837-840
32. D C Mishra, G Laxman, M B S V Rao and S B Gupta *Mem Geol Soc India* **31** (1995) 345-352
33. D V Chandrasekhar and D C Mishra *Current Science* **83** (2002) 492-498
34. D V Chandrasekhar, D C Mishra, G V S P Rao and J M Rao *Earth Planet Sci Lett* **201** (2002) 277-292
35. C Subrahmanyam and R K Verma *Tectonophysics* **84** (1982) 225-245
36. D C Mishra, S B Gupta, M B S V Rao, M Venkatrayudu and G Laxman *J Geol Soc Ind* **30** (1987) 469-476
37. A P Singh, D C Mishra, V V Kumar and M B S V Rao *Mem Geol Soc India* **50** (2003) 139-163
38. NGRI (Eds) Bouguer anomaly map of India *Published by National Geophysical Research Institute Hyderabad India* (1975)
39. C Bowin *Mar Geod* **7** (1983) 61-100
40. D V Subba Rao *Current Science* **82** (2002) 1373-1378
41. D Gesch, K L Verdin and S K Greenlee *Eos Trans AGU* **80** (1999) 69-70
42. K L Kaila and V G Krishna *Current Science* **62** (1992) 117-154
43. P R Reddy, N Venkateswarulu, P K Rao and A S S S R S Prasad *Current Science* **77** (1999) 1606-1611
44. M R Kumar, J Saul, D Sarkar, R Kind and A K Shukla *Geophys Res Lett* **28** (2001) 1339-1342
45. D D Singh *Tectonophysics* **139** (1987) 187-203
46. A R Lowry and R B Smith *J Geophys Res* **99** (1994) 20123-20140
47. D J Thomson *Proc IEEE* **70** (1982) 1055-1096
48. F Simpson *Geofluids* **1** (2001) 123-136
49. C J Swain and J F Kirby *Geop Res Lett* **30** (2003) 1574 doi:10.1029/2003GL017070
50. D Slepian *Bell Syst Tech J* **57** (1978) 1371-1429
51. A R Lowry and R B Smith *J Geophys Res* **100** (1995) 17947-17963
52. T N Gowd, S V R Rao and V K Gaur *J Geophys Res* **97** (1992) 11879-11888
53. G Barruol and R Hoffmann *J Geophys Res* **104** (1999) 10757-10773
54. A Maggi, J A Jackson, D McKenzie and K Priestley *Geology* **28** (2000) 495-498
55. B R Rao *Tectonophysics* **201** (1992) 175-185
56. H K Gupta, S V S Sarma, T Harinarayana and G Virupakshi *Geophy Res Lett* **23** (1996) 1569-1572
57. S N Rai, S Thiagarajan and D V Ramana *Current Science* **85** (2003) 208-213
58. K Rajendran and C P Rajendran *Current Sci* **85** (2003) 896-903